Paper

Parameter Optimization on the Fabrication of Al-10Si-0.4Mg Alloy Using Selective Laser Melting Process

Masahiro ARAKI[1], Shinnosuke KUSAKAWA[2], Kazuhiro NAKAMURA[1], Makiko YONEHARA[3], Toshi-Taka IKESHOJI[3] and Hideki KYOGOKU[4]*

[1]Kindai University Hiroshima Branch, Technology Research Association for Future Additive Manufacturing, 1 Takaya-Umenobe, Higashihiroshima 739-2116, Japan.
[2]Dept. Robotics, Kindai University (Present, Daifuku Co. Ltd.), 1 Takaya-Umenobe, Higashihiroshima 739-2116, Japan.
[3]Research Institute of Fundamental Technology for Next Generation, Kindai University, 1 Takaya-Umenobe, Higashihiroshima 739-2116, Japan.
[4]Dept. Robotics, Kindai University, 1 Takaya-Umenobe, Higashihiroshima 739-2116, Japan.

Received November 23, 2017; Revised January 16, 2018; Accepted January 24, 2018

ABSTRACT

Additive Manufacturing (AM) technology has advantages in building free shape and simplification of manufacturing process. In order to manufacture the high quality parts, it is important to find out the optimum fabrication parameters such as laser power, scan speed, scan pitch and so on. In this research, the fabrication conditions under high power and high scan speed were investigated to fabricate the sound parts of Al-10Si-0.4Mg alloy using a SLM machine equipped with a 1 kW single mode fiber laser. As a result, the effective process window in the process map of the laser power and the scan speed was found out by evaluating the density of the specimens. The range of the energy density that showed high relative density of the parts was 35~80 J/mm^3, and it was similar to the result reported by other researches. In the case of the laser power of 700 W, it was found that the relative density keeps high value even at a scan speed of 2200 mm/s. Thus, it was found that the sound parts can be fabricated at high scan speed by increasing the laser power. And the optimum scan pitch was similar to the laser spot size.

KEY WORDS

Additive Manufacturing, selective laser melting, aluminum alloy, parameter optimization, density

1 Introduction

Additive Manufacturing (AM) technology has been dramatically attracting attention as a breakthrough technology in advanced manufacturing because it allows for manufacturing of three-dimensional complex-shaped metallic parts, which are impossible to manufacture using conventional process, through CAD data easily[1)]. Especially, selective laser melting (SLM), which is one of the AM technology, has been widely used in the industrial fields such as aerospace, medical, automotive and so on because SLM is available to fabricate a great variety of alloys such as stainless steel, titanium alloy, aluminum alloy, nickel-based superalloy and so on.

Aluminum alloy is widely applied to the parts of aerospace field, the trial parts of automotive field and so on due to light weight metal. Although it was difficult to fabricate the sound aluminum alloy parts using a SLM machine with CO_2 laser owing to its high reflectivity and high thermal conductivity[2)], it has been able to fabricate the sound parts using a SLM machine with fiber laser. One of the authors[3)] tried to fabricate the sound parts using a SLM prototype machine with 50 W fiber laser in 2007, but it was difficult to fabricate high-density aluminum alloy parts. Recently, since the commercial SLM machines have been equipped with a high power fiber laser, the high-density parts of Al-10Si-0.4Mg alloy have been able to fabricate. Therefore, there are many reports[4-14)] on the fabrication of the alloy using SLM machines.

Kempen et al.[5)] reported that the density of Al-10Si-0.4Mg alloy fabricated using a SLM machine with 200 W fiber laser and irregular shaped powder was around 93%. And also, Kempen et al.[12)] found the optimum fabrication conditions by making the process map of single track by changing the laser power between 170 W and 200 W and the scan speed between 200 mm/s and 1400 mm/s using a SLM machine with 200 W fiber laser. Kimura et al.[8)] found the optimum fabrication condition, by which can be obtained the almost full density parts, by investigation of the laser power between 200 W and 370 W and the scan speed between 400 mm/s and 3000 mm/s using a SLM machine with 400 W fiber

* Corresponding author, E-mail: kyogoku@hiro.kindai.ac.jp
** The content of this article had been presented at JSPMIC2017.

laser. Although the high speed fabrication of the parts is strongly demanded in the AM technology, it is difficult to achieve it due to lower laser power and other limitation.

In this research, the fabrication conditions were investigated under high power and high scan speed to fabricate the sound parts of Al-10Si-0.4Mg alloy using the SLM machine equipped with a 1 kW single mode fiber laser developed in the METI project.

2 Experimental procedures

2.1 Fabrication conditions

The SLM prototype machine equipped with a 1 kW single mode fiber laser was employed for fabricating the specimens. The specification of the machine is as follows;

- Laser: 1 kW single mode fiber laser (wave length: 1.07 μm)
- Scan speed: max. 5000 mm/s
- Build size: 250 × 250 × 180 mm

The gas-atomized Al-10Si-0.4Mg powder which is irregular shape as shown in Fig. 1 was prepared in this research. The chemical composition of this powder is given in Table 1. The average diameter of the powder is 53.3 μm at D50 as shown in Table 2.

In order to examine the optimum fabrication condition, the cubic specimens with the dimension of 16.4 × 12.4 × 15.0 mm were fabricated under the following conditions as shown in Fig. 2.

- Laser power: 300, 500, 700 W

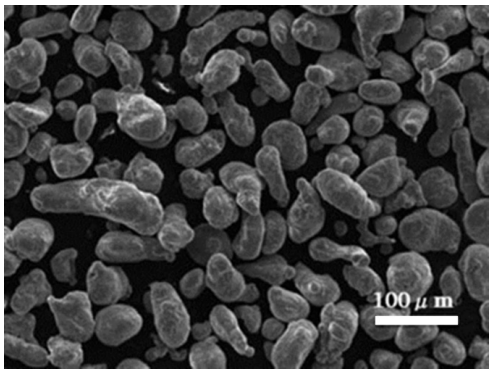

Fig. 1 SEM image of Al-10Si-0.4Mg alloy powder.

Table 1 Chemical composition of Al-10Si-0.4Mg alloy powder.

Chemical composition [mass%]									
Cu	Fe	Si	Mn	Mg	Zn	Ni	Cr	Ti	Al
0.02	0.15	10.19	0.01	0.37	Tr	0.01	Tr	0.01	Bal.

(Tr: <0.01%)

Table 2 Particle distribution of Al-10Si-0.4Mg alloy powder.

D10%	D50%	D90%
37.9 μm	53.3 μm	79.8 μm

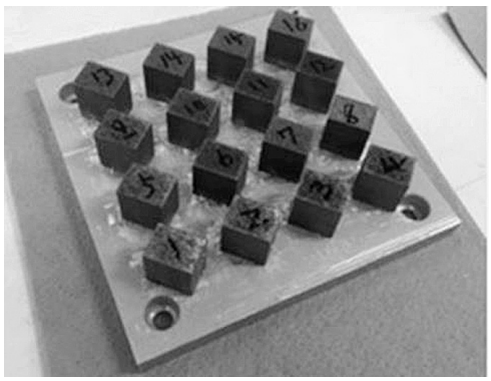

Fig. 2 Cubic specimens of Al-10Si-0.4Mg alloy fabricated under various conditions of laser power and scan speed.

- Scan speed: 510～3205 mm/s
- Scan pitch: 0.1~0.32 mm
- Layer thickness: 0.05 mm
- Spot diameter: 0.1 mm

2.2 Examination of the specimens

The density of the as-built specimens was measured by the Archimedes method. The relative density was calculated using the reference value for the density, 2.67 g/cm^3. The microstructure was observed using an optical microscope (OM) and a scanning electron microscope (SEM). And also the element analysis was performed by EDS and crystallographic orientation by EBSD. The melting and solidification behavior was observed using a high-speed camera and a thermo-viewer.

3 Results and discussions

3.1 Process map

In order to manufacture the sound parts, it is very important to find out the optimum fabrication conditions. Especially, laser power, scan speed, scan pitch, and layer thickness are significant process parameters. And also, the energy density, E, calculated by the following equation[15] is used as a significant factor;

$$E = P/vst \quad (1)$$

where P: laser power [W], v: scan speed [mm/s], s: scan pitch [mm], and t: layer thickness [mm].

At first, the process map between the laser power and the scan speed was made by measurement of density of the as-built cubic specimens. As shown in Fig. 3, the density was classified into three types as follows;

○: ≧99%, △: <99%, ≧98%, ×: <98%

The suitable fabrication condition is determined by the shading area in this process map. It is found from this process map that the high density parts can be fabricate even in the case of higher laser power and higher scan speed. Thus, it was found that the high density part of more than 99% can be fabricated at the laser power of 700 W up to the scan speed of 2200 mm/s.

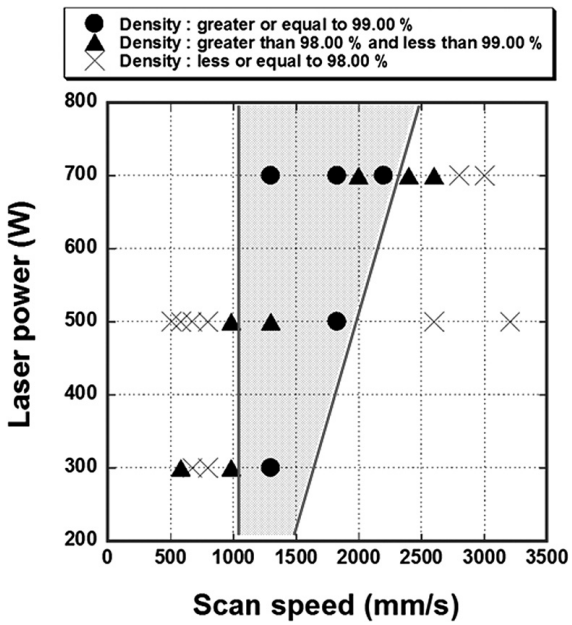

Fig. 3 Process map of Al-10Si-0.4Mg alloy drawn by evaluating the density.

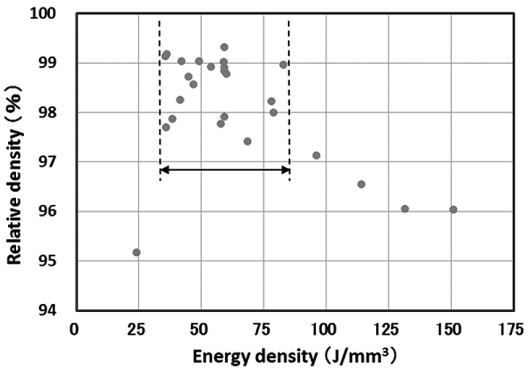

Fig. 4 Variation in the relative density of the as-built alloy as a function of energy density.

3.2 Effect of energy density on the density of the parts

As mentioned above, the energy density, which is very important factor, strongly affects the density of the as-built parts. The relation between the energy density and the relative density is shown in Fig. 4. Although the deviation of the relative density was greater, the range of more than 99% in the relative density almost corresponds to the range from 35 to 80 J/mm^2 in the energy density. This result is similar to that reported by Kimura et al.[8] And also the relative density of the parts is 99~99.4%, which is similar to that of the parts fabricated using irregular shaped powder reported by Kempen et al.[5] While, Kimura et al.[8] reported that the relative density of the parts fabricated using spherical powder is almost full density. Thus, one of the reasons of lower density in our research is considered to be owing to irregular shaped powder. And also, another reason may be due to the thicker layer thickness of 50 μm, as Qiu et al.[16] reported that the porosity increases rapidly above 40 μm in powder layer thickness. In the cases of both lower energy density and higher energy density, the relative density decreased.

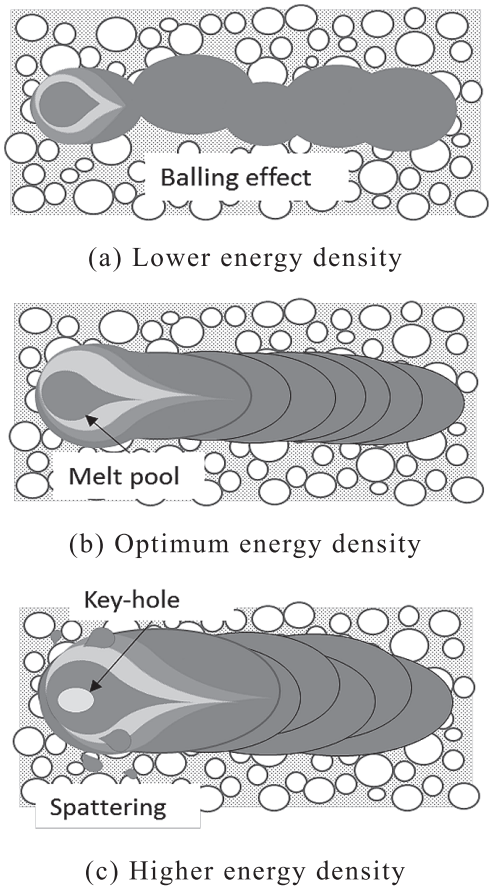

Fig. 5 Schematic of melting and solidification behavior.

Even in the case of the energy density between 35 and 80 J/mm^3, the relative density deviates and is less than 99% in many cases. This is because the relative density was affected by the scan pitch, especially in the case of the larger scan pitch it deviated widely.

The melting and solidification behavior by laser radiation was investigated by the simulation and the experiments using a high speed camera[16-19]. Khairallah et al.[17] revealed how the strong dynamical melt flow by recoil pressure and Marangoni convection generates pore defects, spattering, and denudation zones using three-dimensional high fidelity powder-scale model. And also, Qiu et al.[16] described that the formation of pores and development of rough surface are strongly associated with unstable melt flow and spattering. The melting and solidification behavior can be proposed by these reports and our observation using a high speed camera and a thermo-viewer as the schematic as shown in Fig. 5. In the case of lower energy density as shown in Fig. 5 (a), large pores form mainly due to balling effect. In the case of the optimum energy density, a few faults form because of stable melt pool and a few spattering as shown in Fig. 5 (b). On the other hand, in the case of higher energy density, a lot of pores and faults form mainly because of the trap of argon gas by great waving of the melt pool due to Marangoni convection and the defects of the powder bed by spattering as shown in Fig. 5 (c) and Fig. 6. Kimura et al.[8] reported

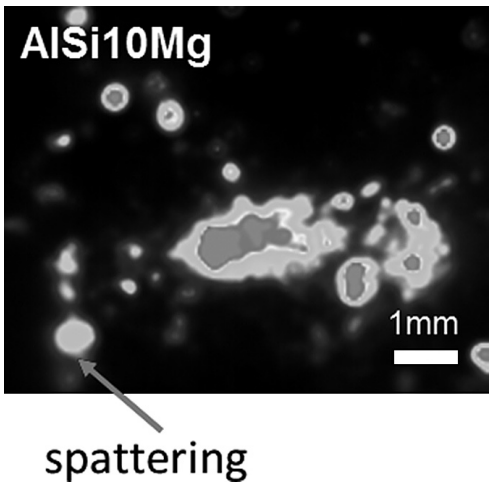

Fig. 6 An example of spattering behavior during laser radiation.

that the trapped gas in pores is consisted of argon gas and hydrogen by analyzing the gas. Since our experiment was carried out in the similar atmosphere, the gas in pores may be consisted of argon gas and hydrogen.

Fig. 7 shows the variation in the relative density of the as-built alloy as a function of energy density at a laser power of 500 W, a scan speed between 500 and 3205 mm/s, a scan pitch of 0.13 mm and a layer thickness of 0.05 mm. The microstructure is also given in the figure. As a result, the relative density is the maximum at a scan speed of 1830 mm/s. In this case, a few very small size pores (black) is observed in Fig. 7 (b). While in the case of the scan speed of 3205 mm/s, that is, lower energy density, a lot of large spherical pores of about 100 μm in size are observed in Fig. 7 (a). This may be because of balling effect due to lower energy density as shown in Fig. 5 (a). On the other hand, in the case of the scan speed of 500 mm/s, that is, higher energy density, a lot of irregular shaped large pores of about 50 μm in size are observed in Fig. 7 (c). This may be because of trapping of gas due to waving of melt pool and spattering from melt pool as shown in Fig. 5 (c).

Thus, it is very important to optimize not only the laser power and the scan speed but also the energy density related these factors in order to fabricate the sound parts. Therefore, the effect of laser power, scan speed and scan pitch on the relative density of the parts were investigated precisely.

3.3 Effects of the laser power and the scan speed on the relative density

The effects of the laser power and the scan speed on the relative density of the parts are investigated at a laser power of 300 W,

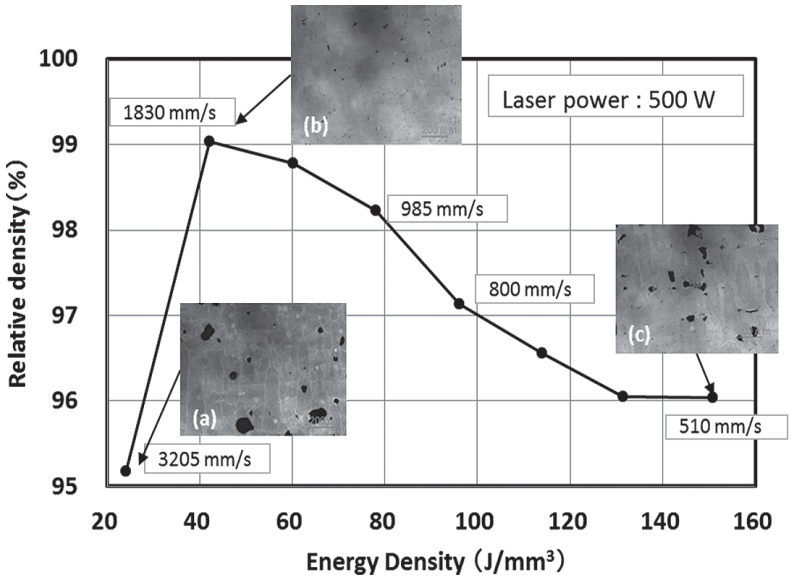

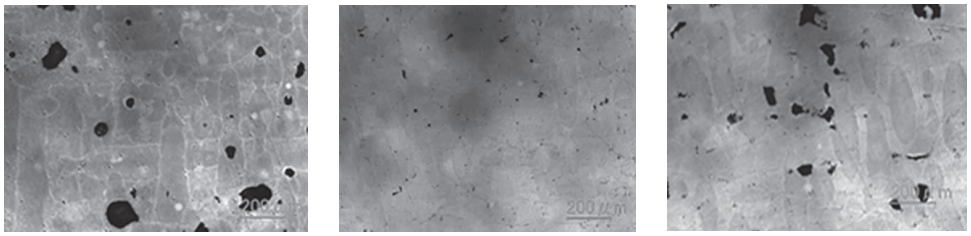

(a) 24 J/mm^3 (b) 42 J/mm^3 (c) 150.8 J/mm^3

Fig. 7 Variation in the relative density of the as-built alloy as a function of energy density at a laser power of 500 W.

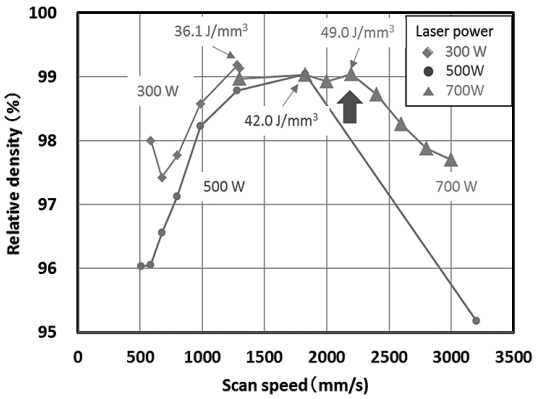

Fig. 8 Variation in the relative density of the as-built alloy as a function of scan speed at a laser power of 500 W.

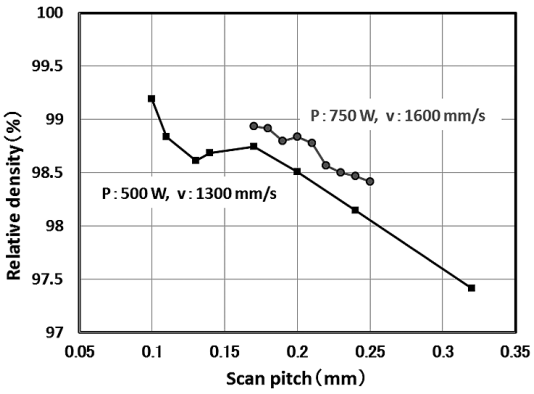

Fig. 9 Variation in the relative density of the as-built alloy as a function of scan pitch at a laser power of 500 W and 750 W.

500 W and 700 W, a scan pitch of 0.13 mm, and a layer thickness of 0.05 mm. Fig. 8 shows the variation in the relative density of the as-built alloy as a function of scan speed at a laser power of 500 W. It was found from this figure that the relative density increases with increasing the scan speed at each laser power, and then shows a plateau region and the maximum, finally decreases with increasing the scan speed. The scan speed showed the maximum relative density depends on the laser power, that is, it becomes slower with decreasing the laser power, while it becomes faster with increasing the laser power. The energy density showed the maximum relative density is denoted in the figure, and it becomes higher with increasing the laser power. According to other researches[5,8,12] carried out at a laser power between 200 W and 400 W, it was reported that the relative density becomes the maximum around 300 W[8]. As shown in Fig. 8, in the case of the laser power of 700 W, the relative density keeps high value even at a scan speed of 2200 mm/s. Qui et al.[16] reported that the high density parts of Ti-6Al-4V is able to fabricate at a laser power of 400 W even at a scan speed of 2700 mm/s. Thus, it was found that higher laser power make the fabrication of sound parts under higher scan speed possible.

3.4 Effect of the scan pitch on the relative density of the parts

Fig. 9 shows the variation in the relative density of the as-built alloy as a function of scan pitch at a laser power of 500 W and 750 W. The relative density increases with decreasing the scan pitch, and, in the case of 500 W and 1300 mm/s, it becomes the maximum at a scan pitch of 0.1 mm. The microstructure of the specimen fabricated at a scan pitch of 0.1 mm shows a few pores similar to that of Fig. 7 (b). On the other hand, in the case of a scan pitch of 0.32 mm, a lot of large pores observed. As mentioned above, this may be because powder was not able to be melted enough due to lower energy density. Thus, it was found that the optimum scan pitch is similar to the laser spot size.

4 Conclusions

In this research, the fabrication conditions under high power and high scan speed were investigated to fabricate the sound parts of Al-10Si-0.4Mg alloy using the SLM machine equipped with a 1 kW single mode fiber laser. The results obtained are as follows;

(1) The effective process window in the process map of the laser power and the scan speed was found out by evaluating the density of the specimens.

(2) The range of the energy density that showed high relative density of the parts was 35~80 J/mm^3, and it is similar to the result reported by other researches.

(3) In the case of the laser power of 700 W, it was found that the relative density keeps high value even at a scan speed of 2200 mm/s. Thus, it was found that higher laser power make the fabrication of sound parts under higher scan speed possible.

(4) It was found that the optimum scan pitch is similar to the laser spot size.

Acknowledgement

This work was performed in the Ministry of Economy, Trade and Industry “Next generation industrial 3D printer technology project” by Technology Research Association for Future Additive Manufacturing (TRAFAM).

References

1) H. Kyogoku: J. Jpn. Soc. Precision Engineering, **82** (2016) 619-623.
2) T. B. Sercombe, G. B. Schaffer: Science, **30** (2003) 1225-1227.
3) H. Kyogoku, M. Hagiwara, T. Shinno: Solid Freeform Fabrication Proceedings 2010, Austin TX, (2010) 140-148.
4) K. Barkowiak, S. Ullrich, T. Frick, M. Schmidt:Physics Procedia, **12** (2011) 393-401.
5) K. Kempen, L. Thijs, J. Van Humbeeck, J.-P. Kruth: Physics Procedia, **39** (2012) 439-446.
6) E. Louvis, P. Fox, C. J. Sutcliffe: J. Materials Processing Technology, **211** (2011) 275-284.
7) E. Brandle, U. Heckenberger, V. Holzinger, D. Buchbinder: Materials and Design, **34** (2012) 159-169.

8) T. Kimura, T. Nakamoto: J. Jpn. Soc. Powder Powder Metallurgy, **61** (2014) 531-537.
9) A. Mertens, O. Dedry, D. Reuter, O. Rigo, J. Lecomte-Beckers: Solid Freeform Fabrication Proceedings 2015, Austin TX, (2015) 1007-1016.
10) T. Kimura, T. Nakamoto: J. Jpn. Inst. Light Metals, **66** (2016) 167-173.
11) X. P. Li, X. J. Wang, M. Saunders, A. Suvorova, L. C. Zhang, Y. J. Liu, M. H. Fang, Z. H. Huang, T. B. Sercombe: Acta Materialia, **95** (2015) 74-82.
12) K. Kempen, L. Thijs, J. Van-Humbeeck, J.-P. Kruth: Materials Science and Technology, **31** (2015) 917-923.
13) T. Kimura, T. Nakamoto; Materials and Design, **89** (2016) 1294-1301.
14) C. E. Roberts, D. L. Bourell, T. Watt, J. Cohen: Physics Procedia, **83** (2016) 909-917.
15) A. Simchi: Materials Science & Engineering A, **428** (2006) 148-158.
16) C. Qiu, C. Panwisawas, M. Ward, H. C. Basoalto, J. W. Brooks, M. M. Attallah: Acta Materialia, **96** (2015) 72-79.
17) S. A. Khairallah, A. T. Anderson, A. Rubenchik, W. E. King: Acta Materialia, **108** (2016) 36-45.
18) T.-T. Ikeshoji, H. Kyogoku, M. Yonehara, M. Araki, K. Nakamura: Proceedings of the 27th Annual International Solid Freeform Fabrication Symposium (CD-ROM), Austin, TX(2016).
19) M. J. Matthews, G. Guss, S. A. Khairallah, A. M. Rubenchik, P. J. Depond, W. E. King: Acta Materialia, **114** (2016) 33-42.